Unique Antimicrobial Effects of Platelet-Rich Plasma and Its Efficacy as a Prophylaxis to Prevent Implant-Associated Spinal Infection

*Hongshuai Li, Therwa Hamza, John E. Tidwell, Nina Clovis, and Bingyun Li**

Platelet-rich-plasma (PRP) has attracted great attention and has been increasingly used for a variety of clinical applications including orthopedic surgeries, periodontal and oral surgeries, maxillofacial surgeries, plastic surgeries, and sports medicine. However, very little is known about the antimicrobial activities of PRP. PRP is found to have antimicrobial properties both in vitro and in vivo. In vitro, the antimicrobial properties of PRP are bacterial-strain-specific and time-specific: PRP significantly (80-100 fold reduction in colony-forming units) inhibits the growth of methicillin-sensitive and methicillin-resistant Staphylococcus aureus, Group A streptococcus, and Neisseria gonorrhoeae within the first few hours but it has no significant antimicrobial properties against E. coli and Pseudomonas. The antimicrobial properties of PRP also depend on the concentration of thrombin. In vivo, an implant-associated spinal infection rabbit model is established and used to evaluate the antimicrobial and wound-healing properties of PRP. Compared to the infection controls, PRP treatment results in significant reduction in bacterial colonies in bone samples at all time points studied (i.e. 1, 2, and 3 weeks) and significant increase in mineralized tissues (thereby better bone healing) at postoperative weeks 2 and 3. PRP therefore may be a useful adjunct strategy against postoperative implant-associated infections.

1. Introduction

Infection is a significant clinical complication in spinal-implant surgeries and other injuries (e.g., open fractures) and a variety of surgeries.[1,2] Despite improvements in surgical techniques, systemic antibiotic prophylaxis, and reduced operating time, the rate of spinal implant-associated postoperative infection could still be up to 8.5% and higher, depending on patient- and procedure-related factors.[3] Patients who are elderly, immunocompromised, diabetic, obese, cognitively impaired, or sustain trauma have greater risks of infection after spinal surgery.[2,4] Apart from patient discomfort, the cost of treating a single implant-associated spinal wound infection could be more than $900,000.[5] Therefore, prevention of spinal implant-associated infection is important in the battle against rising healthcare costs.

Platelet-rich plasma (PRP) is a portion of autologous blood that contains concentrated platelets and leukocytes. A 2009 article in *The New York Times* raised public awareness of PRP by detailing the use of PRP to treat an injured Pittsburgh Steelers football player before the 2009 Superbowl.[6] PRP has been used for clinical applications in a variety of orthopedic surgeries, periodontal and oral surgeries, maxillofacial surgeries, plastic surgeries, sports medicine, etc.[7] Applications of PRP by itself[8] or in combination with other biomaterials[9] are also attracting attention in spinal arthrodesis.

Despite the large number of recent publications on PRP's potential wound-healing properties, little is known about its antimicrobial activity;[10,11] a few recent clinical studies have indicated that PRP may also have strong antimicrobial properties. Trowbridge et al.[12] and Englert et al.[13] showed improved wound healing and decreased infection rate following cardiac surgeries when PRP was applied during sternum closure. Yuan et al.[14] reported improved outcome in treating chronic femoral osteomyelitis with topical usage of PRP. The reported antimicrobial properties of PRP may be associated with the capability of platelets to store and process antimicrobial proteins. Two platelet-derived components in serum were found to be associated with the antimicrobial activity of platelets toward Bacillus subtilis.[15] Donaldson and colleagues[16] isolated a bactericidal protein (β-lysin) that is stored at high concentrations in rabbit platelets and to a lesser extent in human platelets. Nachman and Weksler[17] and Yeaman et al.[18,19] isolated and characterized platelet microbicidal proteins in rabbits and humans. Krijgsveld et al.[20] reported bactericidal proteins in human

H. Li, T. Hamza, J. E. Tidwell, N. Clovis, Prof. B. Li
Department of Orthopaedics, School of Medicine
West Virginia University
Morgantown, WV 26506, USA
E-mail: bili@hsc.wvu.edu
H. Li
Department of Orthopaedics
University of Pittsburgh
Pittsburgh, Pennsylvania 15219, USA
Prof. B. Li
WVNano Initiative, Morgantown, WV 26506, USA
Prof. B. Li
Mary Babb Randolph Cancer Center, Morgantown, WV 26506, USA

DOI: 10.1002/adhm.201200465

platelets that are released upon thrombin stimulation. The purposes of this study are i) to determine the in vitro antimicrobial effects of PRP against six bacterial isolates commonly found in bone infections, ii) to establish a spinal-implant-associated animal model that allows both infection and healing evaluations, and iii) to examine in vivo whether PRP could be used alone as a prophylaxis for spinal-implant-associated infection.

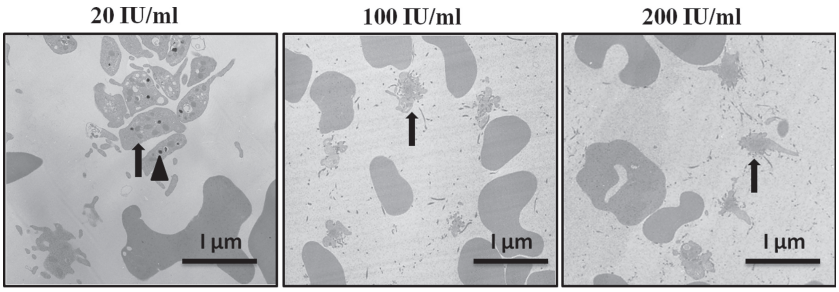

Figure 1. Ultrastructure of PRP activated by thrombin of different concentrations. PRPs were activated for 5 minutes. With increasing thrombin concentration, fewer granules were observed in platelets (↑ indicates platelets and ▲ indicates granules within platelets).

2. Results

2.1. Characterization and Activation of PRP

The prepared PRP had a concentration of 2×10^6 platelets μL^{-1}, which is a significant enrichment (approximately 10 times higher) of platelets compared to the average platelet count in whole blood. Similarly, the leukocyte count increased approximately four fold from the baseline value of $3.20 \pm 0.23 \times 10^3$ leukocytes μL^{-1} in whole blood to $13.51 \pm 0.43 \times 10^3$ leukocytes μL^{-1} in the prepared PRP (**Table 1**).

PRP was activated using thrombin; the higher the concentration of thrombin, the fewer granules were observed within the platelets (**Figure 1**). Five minutes following the addition of thrombin, α granules could still be observed within some platelets at a thrombin concentration of 20 IU mL^{-1} while almost no granules were found at thrombin concentrations of 100 and 200 IU mL^{-1} (Figure 1).

2.2. In Vitro Antimicrobial Effects of PRP against Six Clinical Bacterial Isolates

The cultures that contained PRP gel showed a distinct decrease in colony-forming unit (CFU) counts of methicillin-sensitive Staphylococcus aureus (MSSA), methicillin-resistant Staphylococcus aureus (MRSA), Group A Streptococcus, and Neisseria gonorrhoeae in the first 2 h compared to the controls; their maximum decrease in CFU counts were approximately 100-, 97.5-, 95-, and 80-fold, respectively (**Figure 2**A–D). All concentrations (i.e., 20, 100, and 200 IU mL^{-1}) of thrombin led to a significant ($p < 0.01$) decrease of CFU counts in MSSA (1 and 2 h), MRSA (2 h), and Group A. Streptococcus (1 h) compared to the control; the higher the concentration of thrombin, the lower the CFU counts (Figure 2A–C). Only a high concentration (i.e., 200 IU mL^{-1}) of thrombin resulted in a significant reduction of CFU count in Neisseria gonorrhoeae within the first 2 h (Figure 2D). At all concentrations of thrombin studied, no significant decrease in CFU count was observed in the Pseudomonas and E. coli cultures (Figure 2E and F). Meanwhile, no significant reduction of CFU count was found in cultures containing platelet-poor plasma (PPP) gels that were activated with the three thrombin concentrations (i.e., 20, 100, and 200 IU mL^{-1}) compared to the control (Figure 2A–F). However, for all bacterial isolates, the CFU counts started to increase substantially at 4 h and reached a plateau at approximately 12 to 24 h (Figure 2A–F).

The bacteria in the PRP-gels were also examined in the MSSA cultures (Supplementary Figure 1). Barely any bacteria (1.67 ± 2.08) were detected in the PRP gel at 1 h, and the CFU counts within the PRP gels increased with time. However, the CFU counts within the PRP gels were substantially (at least 100 times) less than those of the supernatants at all time-points tested. In addition, PRP had similar antimicrobial effects against S. aureus (ATCC 25923, ATCC, Manassas, VA) and the clinical isolate MSSA.

Table 1. Platelet and leukocyte counts in PRP and whole blood.

	Whole blood	PRP
Platelets [10^5 μL^{-1}]	1.98 ± 0.22	20.50 ± 1.32[a)]
Leukocytes [10^3 μL^{-1}]	3.20 ± 0.23	13.51 ± 0.43[a)]

[a)] $p < 0.001$ compared to whole blood.

2.3. In Vivo Efficacy of PRP in Preventing Postoperative Implant-Associated Spinal Infection

2.3.1. General Observations

After surgery, animals started to gain weight at postoperative day 5. The surgical sites of those without bacterial challenges (sham control) were clear of infection at all time-points studied (**Figure 3**A). By contrast, the surgical sites with bacterial challenges had elevated bumps; the bumps were relatively smaller for PRP treatment sites than for infection control sites (Figure 3B). Significant amounts of pus were found in all bacterially challenged surgical sites (Figure 3C), which indicates severe infection.

2.3.2. Microbiological Evaluation

No bacterial growth was detected in any blood samples or samples from the sham control sites (data not shown), which indicates that there was no systemic infection. Postmortem quantification of bacteria in surgical sites challenged with bacteria showed high burdens [on the order of 10^6 or 10^7 CFU (g tissue)$^{-1}$] in both bone and muscle cultures (**Figure 4**). Compared to the infection control sites, PRP treatment sites had

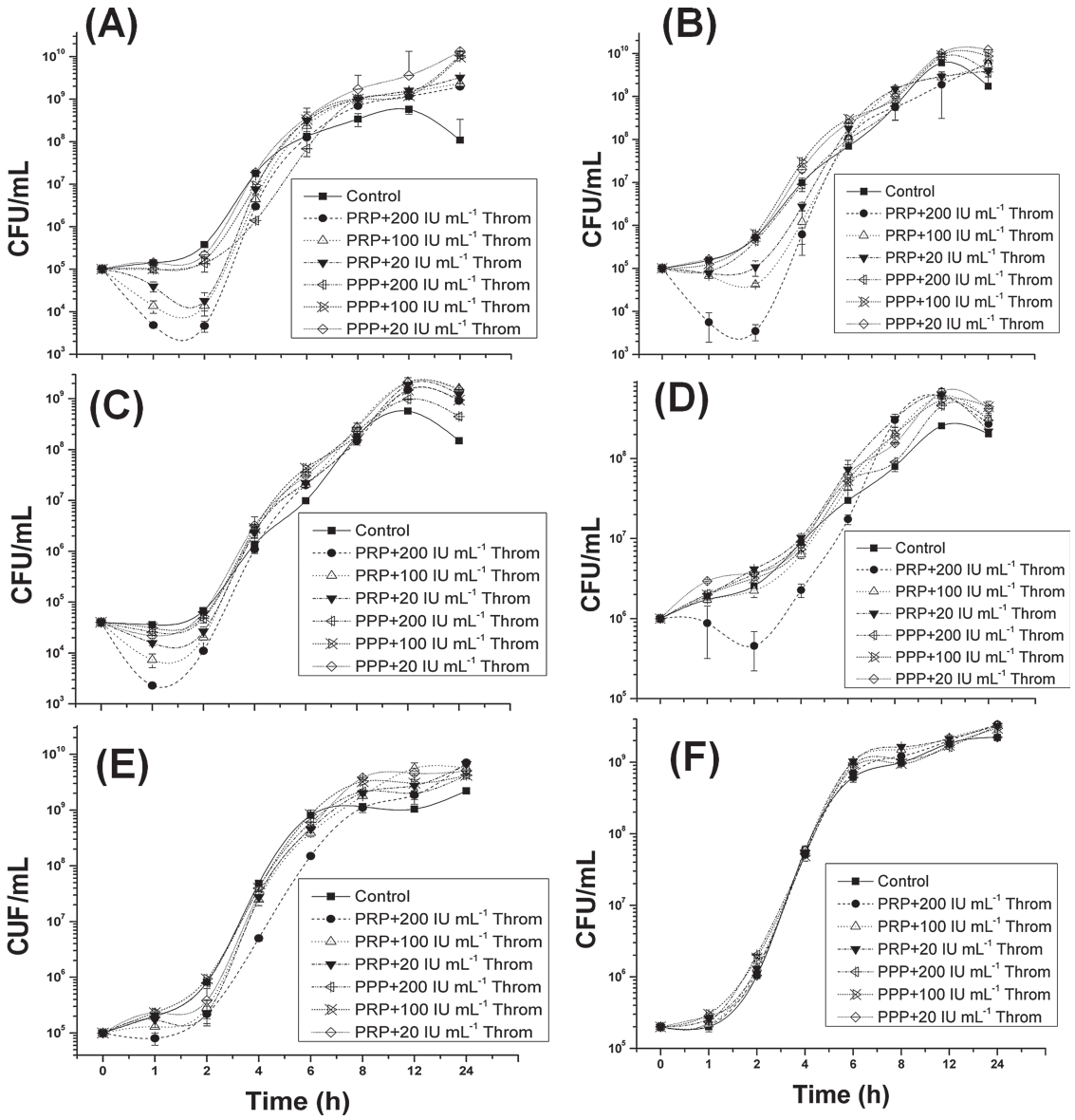

Figure 2. In vitro antimicrobial effects of PRP and PPP against A) MSSA, B) MRSA, C) Group A. Streptococcus, D) Neisseria gonorrhoeae, E) Pseudomonas, and F) E. coli.

significantly fewer bacterial colonies in bone samples at all time-points studied (i.e., 1, 2, and 3 weeks) and in muscle samples at weeks 1 and 2 (Figure 4A and B). Clear differences in the number of bacterial colonies were also observed from the Kirschner-wire (K-wire) rolling experiments; fewer colonies were found in the PRP treatment sites than at the infection control sites (Figure 4C).

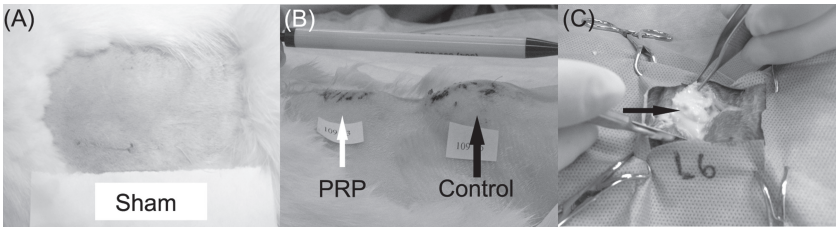

Figure 3. General observation at postoperative week 3. A) Sham control site without bacterial challenge: no signs of infection were found. B) Surgical sites (white arrow denotes a PRP treatment site and black arrow denotes an infection control site) with bacterial challenges: signs of local infection were observed. C) Typical surgical site with bacterial challenges: black arrow highlights pus.

2.3.3. Histopathological Examination

Vertebral samples from infected surgical sites at the study end-point (i.e., postoperative week 3) were used to confirm the presence of infection by hematoxylin and eosin (H&E) staining. Chronic inflammatory cell infiltration, osteolysis, and clusters of bacteria were observed at postoperative week 3 in the infection control sites, while relatively less inflammatory cell infiltration and fewer

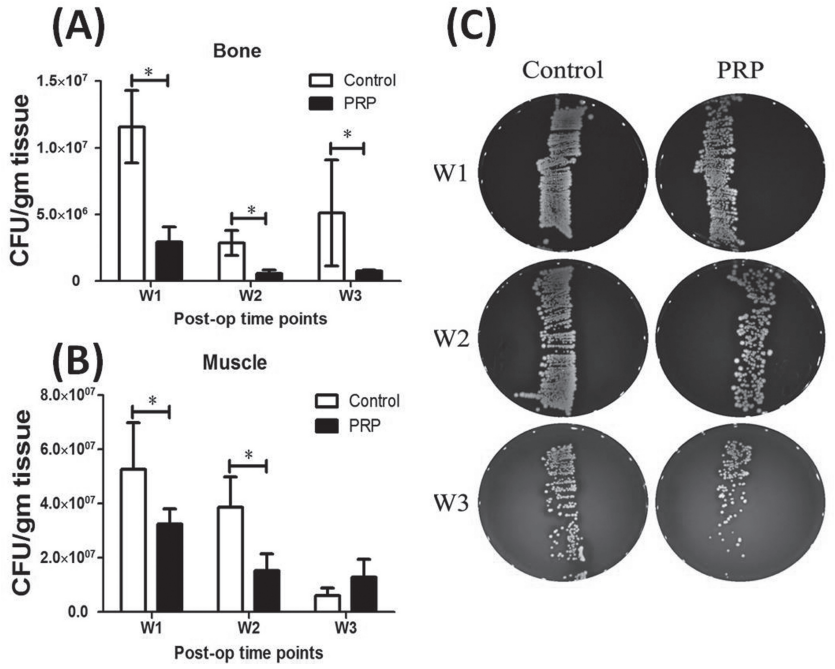

Figure 4. Microbiological evaluation of local A) bones, B) muscles, and C) K-wires. $*p < 0.05$ compared to the infection control.

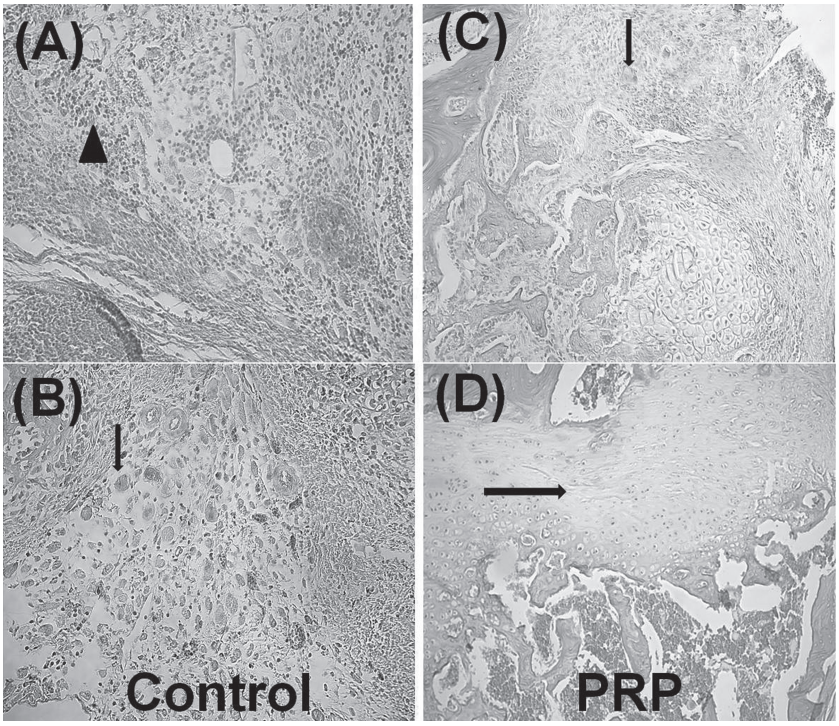

Figure 5. Histological examination of the defect areas at postoperative week 3. A) and B): infection control site; C) and D): PRP treatment site. H&E staining with 20× magnification. Chronic inflammatory cell infiltration (▲) and clusters of bacteria (↓) were found in the infection control sites while less inflammatory cell infiltration and more new bone formation (→) were observed in the PRP treatment sites.

clusters of bacteria were seen in the PRP treatment sites (**Figure 5**).

2.3.4. Bone-Healing Evaluation

By examining 3D reconstructions of the defect areas, we found that the size (diameter and depth) of the bone defects was larger at postoperative week 3 than at week 1 for the infection control sites, while the bone-defect size was much smaller for the PRP treatment sites at postoperative week 3 than at week 1 (**Figure 6**A). Correspondingly, the volume of mineralized tissue within the defined region of interest (ROI) decreased from postoperative week 1 to week 3 for the infection control sites, which indicates bone desorption or destruction. By contrast, the volume of mineralized tissue within the defined ROI increased from postoperative week 1 to 3 for the PRP treatment sites (Figure 6B). No significant difference in the volume of mineralized tissue was found between the infection control site and the PRP treatment site at postoperative week 1, while significant differences were seen at postoperative weeks 2 and 3, whereby more mineralized tissue was detected in the PRP treatment sites than in the infection control sites (Figure 6B). In addition, no significant differences were observed in the volume of mineralized tissue between the sham control and the PRP treatment groups at all time-points studied (Figure 6B).

3. Discussion

PRP contains over 30 growth factors[21] and has been utilized in surgery for about two decades[7,15] with commercially available products.[22] Meanwhile, platelets are known to store and process quite a few antimicrobial proteins.[15–20] However, very little is known about the potential antimicrobial properties of PRP. In this study, we examined the antimicrobial properties of PRP both in vitro and in vivo. To our knowledge, this study is the first in vivo study using autologous PRP for the treatment of implant-associated spinal infection.

In vitro, we tested six clinical bacterial isolates that are commonly found in bone infections.[23] We found that PRP has some antimicrobial effects against MSSA, MRSA, Group A. Streptococcus, and Neisseria gonorrhoeae, and no significant antimicrobial effects against E. coli and Pseudomonas. We

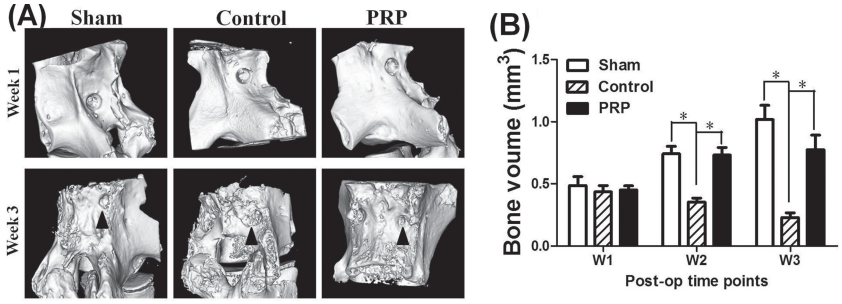

Figure 6. Micro-computed tomography (CT) analysis of mineralized tissues surrounding the bone defects of laminas. A) Representative 3D reconstruction of lumbar spine showing defects; sham sites showing natual bone healing; the infection control sites (control) showing an enlarged defect area; while PRP treatment groups show a smaller defect area (▲ points out the defects). B) Bone volume surrounding the bone-defect areas shows decreased mineralized tissues in the infection control sites compared to the sham control sites, and increased bony tissues in the PRP treatment sites compared to the infection control sites at postoperative weeks 2 and 3. $^{*}p < 0.01$ compared to the infection control group.

found that PRP could significantly (80–100 fold reduction in CFUs at 200 IU mL^{-1} thrombin) inhibit the growth of MSSA, MRSA, Group A. Streptococcus, and Neisseria gonorrhoeae within the first 2 h (Figure 2). This finding was consistent with the literature, where Bielecki et al.[11] found that human PRP could inhibit the growth of MSSA and MSRA. In their study, however, PRP also inhibited the growth of E. coli, which was not seen herein. This inconsistency may be related to the differences in the bacterial species and testing approaches; compared to the kill-curve assay, their Kirby-Bauer disc-diffusion method may allow for the observation of relatively weak antimicrobial performance.

In this study, however, the antimicrobial effects of PRP seem to be limited: The maximum decrease (up to 100-fold) in bacteria (MSSA, MRSA, Group A Streptococcus, and Neisseria gonorrhoeae) was seen within the first 2 h (Figure 2A–D), after which the growth of bacteria exceeded the killing effects, and the number of bacteria started to increase until the stationary phase was reached. We also found that PPP and thrombin do not have antimicrobial properties. However, the concentration of thrombin played a role in the antimicrobial properties of PRP; the higher the thrombin concentration (over the range of 20 to 200 IU mL^{-1}), the better the antimicrobial properties (Figure 2). This effect is likely because a higher concentration of thrombin-activated platelets resulted in much faster release of antimicrobial substances from platelets, as evidenced by our transmission electron microscopy (TEM) observations (Figure 1), where fewer α granules were seen with increasing thrombin concentration. Note that an activator like thrombin is needed, in general, to release the platelet contents from PRP, and thrombin concentration was expected to influence the release rates of platelet contents. Besides thrombin, calcium chloride, mechanical stress, and batroxobin, etc., can also be applied for PRP activation.[24–27]

In vivo, the antimicrobial properties of PRP were confirmed in an implant-associated spinal infection rabbit model, where severe infection (Figure 3C) was induced via an inoculum of 10^2 CFU $(100\ \mu L)^{-1}$ MSSA. Note that 100 μL of 10^2 CFU $(100\ \mu L)^{-1}$ S. aureus also induced severe bone infections in an open-fracture rat model,[28] which suggests that 100 μL of 10^2 CFU $(100\ \mu L)^{-1}$ S. aureus is sufficient to induce severe bone infections in a variety of animal models. One advantage of the creation of two surgical sites in one animal is that it reduces the effect of individual differences on the outcomes and also substantially reduces the number of animals used compared to animals with one surgical site. In this study, PRP treatment was found to lead to significantly fewer bacterial colonies in bone samples at postoperative weeks 1, 2, and 3 and in muscle samples at weeks 1 and 2 compared to phosphate-buffered saline (PBS) control treatment (Figure 4A and B). It was not surprising to see fewer differences between PRP treatment and PBS treatment with time increasing from week 1 to week 3, since the in vitro studies showed that PRP has antimicrobial properties against S. aureus in the first few hours (Figure 2A). The in vitro findings may also indicate that more differences between PRP treatment and PBS treatment might be seen earlier than one week. However, in our experimental settings, PRP alone did not completely prevent infection at postoperative week 3. This finding may indicate that more PRP is needed or PRP alone is not sufficient for the prevention of a severe implant-associated infection.

Meanwhile, PRP showed the capability to improve bone healing in the presence of a severe infection. Compared to the PBS control, PRP treatment resulted in smaller bone-defect size (Figure 6A) and more new bone formation at postoperative week 3 (Figure 5D and 6B). The improvement in bone healing with PRP is probably because a large number of growth factors, including but not limited to vascular endothelial growth factors (VEGF), platelet-derived growth factors (PDGF), transforming growth factor-beta (TGF-β), insulinlike growth factor (IGF), and epithelial growth factors (EGF), could be released from platelets upon activation;[29,30] all these growth factors could promote tissue regeneration.

Therefore, we demonstrated both in vitro and in vivo that PRP has some, limited, antimicrobial properties. However, the exact mechanism of the antimicrobial effects of PRP is not yet fully understood. First, PRP contains concentrated platelets (Table 1). Similar to leukocytes, platelets may have three basic bactericidal mechanisms: 1) storing and processing of bactericidal proteins, 2) synthesis of reactive oxygen species (ROS), and 3) phagocytosis. In 1960, Hirsch[31] reported the bactericidal effect of platelets, where bactericidal activities of rabbit serum were observed when platelets were added to the serum but not with addition of leukocytes or erythrocytes. Platelets may also navigate toward inflammatory chemoattractants, express immunoglobulin-G Fc receptors and C3a/C5a complement fragments, and generate antimicrobial oxygen metabolites (e.g., superoxide, hydrogen peroxide, hydroxy free radicals). Moreover, platelets can interact directly with microorganisms, contribute to the clearance of pathogens from the bloodstream, and actively participate in antibody-dependent cell cytotoxicity against microorganisms.[19] Additionally, PRP also contains concentrated leukocytes (Table 1), which may participate in direct bacterial killing (e.g. neutrophil) and antigen-specific

immune responses (e.g., lymphocyte). Finally, it is believed that poor wound healing, systemic malnutrition, tissue hypoxia, compromised skin, and the use of an implant may decrease the host's ability to eliminate bacteria.[32] However, it is not clear whether the improved healing with the use of PRP in this study contributed to the reduction of bacterial presence in the PRP treatment sites.

4. Conclusions

PRP exhibited antimicrobial properties both in vitro and in vivo. In vitro, we found that PRP has antimicrobial properties and that its antimicrobial properties are bacterial-strain-specific: PRP has antimicrobial properties against MSSA, MRSA, Group A. Streptococcus, and Neisseria gonorrhoeae and no significant antimicrobial effects against E. coli and Pseudomonas. The antimicrobial properties of PRP also seemed to be time-specific: PRP significantly (80–100 fold reduction in colony forming units) inhibited the growth of MSSA, MRSA, Group A. Streptococcus, and Neisseria gonorrhoeae within the first few hours, after which the growth of bacteria outpaced its antimicrobial effects. In vivo, we established a spinal implant-associated animal model that allows evaluate of both infection and bone healing, and we found that PRP treatment led to significantly fewer bacterial colonies in bone and muscle samples and significantly more volume of mineralized tissue within bone defects compared to the infection control.

5. Experimental Section

Animal Use: Animal studies were approved by the West Virginia University Institutional Animal Care and Use Committee. 24 female New Zealand white rabbits (2–3 kg each) were used in this study. Six rabbits were used for blood draws for the in vitro antimicrobial tests and 18 were used to create a rabbit spinal infection model for the in vivo antimicrobial studies.

Isolation and Activation of PRP: Whole blood was drawn from rabbits via the ear vein under general anesthesia (inhalation of isoflurane) and mixed with 0.129 mol L^{-1} trisodium citrate (Sigma-Aldrich, Saint Louis, MO). Blood was first centrifuged in a tube at 300 g for 10 min. The supernatant (consisting of plasma, leukocytes, and platelets) and some red blood cells (ca. 1 mm thick below the buffy coat) were transferred into a second tube and centrifuged at 3,000 g for 15 min. Next, the supernatant was collected and used as PPP, and the pellet of platelets and leukocytes at the bottom of the second tube was obtained as PRP. The platelet and leukocyte counts in PRP and whole blood were measured using hemocytometry, and the concentration of platelets in PRP was adjusted to 2.0×10^6 platelets μL^{-1} by adding the necessary volume of PPP.

Bovine thrombin (Thrombin-JMI, King Pharmaceuticals, Inc., Bristol, TN) solutions with 10% calcium chloride were used to activate PRP and PPP. Three concentrations of thrombin (100, 500, and 1000 IU mL^{-1}) in 10% $CaCl_2$ were added to PRP and PPP to form PRP and PPP gels, and the final concentrations of thrombin were 20, 100, and 200 IU mL^{-1}, respectively; the volume ratio of the thrombin solution to PRP or PPP was 1:4.

Bacterial Culture and In Vitro Kill-Curve Assay: Bacterial studies were approved by the West Virginia University Institutional Biosafety Committee. Six bacteria (i.e., MSSA, MRSA, E. coli, Group A Streptococcus, Pseudomonas, and Neisseria gonorrhoeae) that are commonly found in bone infections[23] were examined. The bacteria were clinical isolates obtained from the Clinical Microbiology Lab at West Virginia University Hospitals. The Neisseria gonorrhoeae was cultured and maintained in Eugon broth (Becton, Dickinson and Company, Sparks, MD), and the other isolates were cultured and maintained in Mueller Hinton broth (BBL™, Becton, Dickinson and Company).

The antimicrobial properties of PRP against the six bacterial isolates were examined in vitro using the kill-curve assay.[33] For this assay, 200 µL PBS and 160 µL PRP or PPP were added to sterile polystyrene tubes (Thermo Fisher Scientific Inc.); PBS served as a control. Different concentrations of 40 µL thrombin in 10% $CaCl_2$ was added to the PRP and PPP tubes to form PRP and PPP gels. After gel formation, 1600 µL broth and 200 µL bacteria were added to each tube. Tubes were then incubated at 37 °C with rotation (150 rpm). After 1, 2, 4, 6, 8, 12, and 24 h, samples were mixed by pipette. A 10 µL sample solution was taken from each tube and serial dilutions were made. After brief vortexing, 100 µL solutions from the dilutions were placed on blood agar plates, incubated overnight at 37 °C, and CFUs were determined.

TEM Observations: PRP was prepared and activated as aforementioned with different concentrations of thrombin in 10% $CaCl_2$; the final concentrations of thrombin were 20, 100, and 200 IU mL^{-1}. Five minutes after the addition of thrombin, the PRP gel samples were fixed in 2.5% glutaraldehyde and cut into 1 mm^3 pieces. The samples were subsequently dehydrated and embedded in resin. Sections were

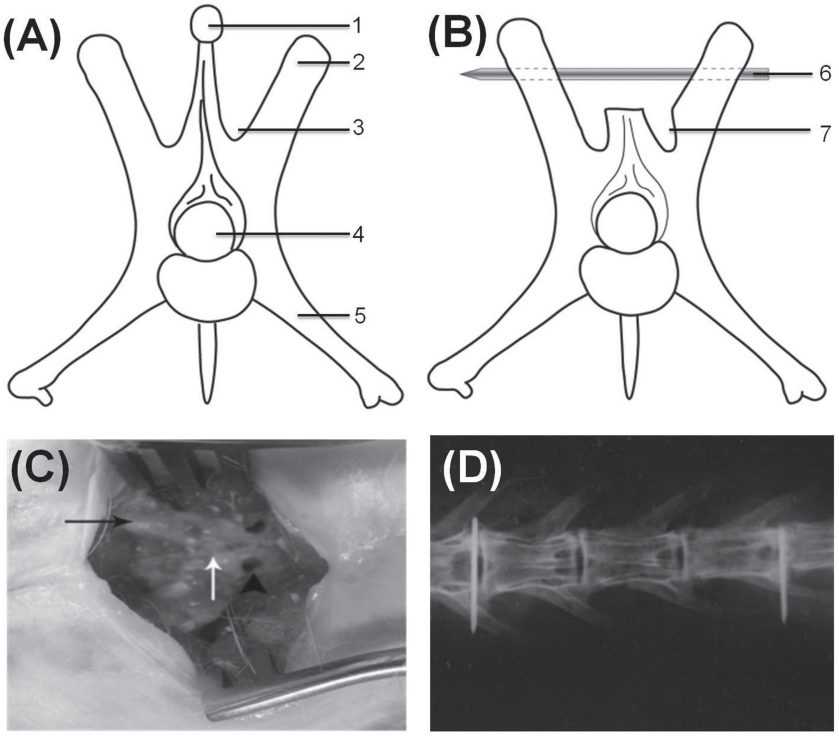

Figure 7. Establishment of a rabbit spinal-implant-associated infection model. Schematic views of rabbit lumber vertebra A) before and B) after surgery. C) Creation of the incision: White arrow shows the base of spinous process (laminectomy); black arrow shows the transverse process; and black triangle shows one of the two defects. D) postoperative radiograph. 1) spinous process; 2) transverse process; 3) laminae; 4) spinal canal; 5) costal process; 6) K-wire; 7) cylinder defects on lamina.

made (70 nm thick) and examined under TEM (JEOL 2000FX, Tokyo, Japan).

Establishment of an Implant-Associated Spinal Infection Model and Treatment with PRP: One day before surgery, S. aureus (ATCC 25923) was suspended in 5 mL trypticase soy broth (BBL™, Becton, Dickinson and Company) and incubated at 37 °C overnight. Immediately before inoculating into the animals, the bacterial concentration was adjusted to 10^2 CFU (100 µL)$^{-1}$ using sterile saline.

An implant-associated spinal infection rabbit model as described by Poelstra et al.[34] was modified by introducing two bone defects (**Figure 7**) to allow bone-healing evaluation. Briefly, rabbits were anesthetized using ketamine (44 mg kg^{-1}) and xylazine (5 mg kg^{-1}) and maintained on isoflurane inhalation anesthesia. Approximately 15 mL of blood was drawn from the ear vein and PRP was prepared as previously described. Two noncontiguous dorsal incisions were made in each rabbit over the L3 and L6 vertebrae (Figure 7C and 7D). The surgical approaches were identical for each incision; separate instruments and drapes were used for each surgical site to prevent cross-contamination. Briefly, the entire spinous process with surrounding muscle and ligament were removed from the base using a rongeur and two bone defects (1.5 mm in diameter and 0.8 in depth, Figure 7C) were created on the two laminas using a slow speed bur with a depth limiter. The ligamentum flavum was not violated and the dura was not exposed. A 0.8-mm diameter stainless steel K-wire (Smith & Nephew, Memphis, TN) was then drilled through both transverse processes and the excess part of the K-wire was cut off (Figure 7B and 7D). Next, a 100-µL S. aureus [10^2 CFU (100 µL)$^{-1}$] inoculum (designated as infection sites) or PBS inoculum (designated as sham control sites) was pipetted onto the K-wire implant and inside the defect pockets. Our previous studies found that 100 µL S. aureus of 10^2 CFU (100 µL)$^{-1}$ was sufficient to induce severe bone infections in animal models.[28] 10 minutes after bacterial inoculation, the infection sites were randomly divided into two groups: the surgical sites in the first group were treated with 100 µL PRP gel activated with thrombin (200 IU mL^{-1}) in 10% $CaCl_2$ and designated as PRP treatment sites, and the sites in the second group were treated with 100 µL PBS and designated as infection control sites. A concentration of 200 IU mL^{-1} thrombin was chosen to activate PRP because this level led to the highest antimicrobial effect against S. aureus in our in vitro studies. PPP did not show significant antimicrobial properties in our in vitro studies therefore PPP was not studied in the animal model. Based on experimental design, the surgical sites were randomly assigned to sham control, infection control, and PRP treatment. Note that autologous PRP was applied to each animal. The fascial and skin incisions were then closed and a radiograph was taken to check positioning of the K-wire.

Postoperatively, 60 mL of physiologic saline was injected subcutaneously to help alleviate any problems from the blood draw. A fentanyl patch was applied (25 µg h^{-1} for 72 h, Sandoz, Princeton, NJ) and was changed after three days to provide six days' worth of analgesia to the rabbits. The animals were housed individually; their incisions and body weight were checked regularly and they were monitored for any signs of sepsis. Animals were euthanized at postoperative weeks 1, 2, and 3 by intracardiac injection of Euthasol euthanasia solution (Virbac Animal Health, Ft. Worth, TX) following a combination of ketamine and xylazine at the same dosage given preoperatively.

Microbiological Evaluation: Before euthanasia, 5 mL blood was drawn and cultured to determine systemic infection. After euthanasia, muscle biopsies surrounding the incision, K-wire (implant), and both transverse processes (bone) were removed, under sterile conditions, from all surgical sites for microbiological evaluation. The remaining whole vertebra (including lamina) was fixed in 10% buffered neutral formalin and used for micro-CT scan and histopathological examination. Harvested muscle and bone tissues were weighed and immediately homogenized in PBS in Ultra-Turrax homogenizer (IKA-Works Inc., Wilmington, NC). Serial dilutions of all samples were made, plated on blood agar plates, and incubated at 37 °C for 24 h. CFUs (gram of tissue)$^{-1}$ were determined. The K-wires were rolled on blood agar plates and incubated for 24 h.

Bone-Healing Evaluation: Before decalcification, the fixed vertebral (including lamina) samples were first scanned with a micro-CT scanner (VivaCT 40, Scanco, Switzerland). All samples were scanned in the coronal plane mounted in a cylindrical sample holder with a current of 0.16 mA, a voltage of 50 kV, and an isotropic resolution of 20 µm (image matrix 1024 × 1024 pixels). Images of defects in both lamina were generated. The three-dimensional trabecular structure of the lamina was reconstructed using the internal software of the Micro-CT. A cylinder region of interest (ROI, 3 mm diameter, 1 mm depth) was created manually in each defect area. Bone volume within the ROI was quantified.

Histopathological Examination: Fixed vertebral samples were decalcified in 10% nitric acid solution for 2 weeks. Samples were paraffin-embedded and 5 µm-thick sections along an axis parallel to the central line of the defects were made. Sections were stained with H&E. A pathologist examined the sections for evidence of acute and chronic infection and evaluated inflammatory cells, osseous destruction, and fibrosis.

Statistical Analysis: Results are expressed as mean ± SD. One-way ANOVA analysis was performed using SPSS 11.0 software (SPSS, Chicago, IL). Statistical significance was set at $p < 0.05$.

Supporting Information

Supporting Information is available from the Wiley Online Library or from the author.

Acknowledgements

The authors acknowledge surgical technical assistance from Suzanne Smith. The authors also acknowledge financial support from the Osteosynthesis and Trauma Care Foundation and National Science Foundation (#1003907). The authors thank John Thomas, PhD for providing the bacterial clinical isolates and John B. Barnett, PhD for his support and the use of the biological safety lab at the Department of Microbiology, Immunology and Cell Biology at West Virginia University. The authors appreciate the use of the transmission electron microscope at the Microscopic Imaging Facilities at the National Institute for Occupational Safety and Health (NIOSH), Morgantown, WV. The authors thank Diane Schwegler-Berry at NIOSH for imaging assistance. Microscope experiments and image analysis were also performed in part in the West Virginia University Imaging Facility, which is supported in part by the Mary Babb Randolph Cancer Center and NIH grant P20 RR016440.

Received: December 14, 2012
Revised: January 16, 2013
Published online:February 27, 2013

[1] R. R. Calderone, D. E. Garland, D. A. Capen, H. Oster, *Orthop. Clin. North Am.* **1996**, *27*, 171.
[2] S. D. Glassman, J. R. Dimar, R. M. Puno, J. R. Johnson, *Spine (Phila Pa 1976)* **1996**, *21*, 2163.
[3] a) A. F. Pull ter Gunne, D. B. Cohen, *Spine (Phila Pa 1976)* **2009**, *34*, 1422; b) A. Veeravagu, C. G. Patil, S. P. Lad, M. Boakye, *Spine (Phila Pa 1976)* **2009**, *34*, 1869; c) W. Zimmerli, A. Trampuz, P. E. Ochsner, *N. Engl. J. Med.* **2004**, *351*, 1645; d) M. A. Weinstein, J. P. McCabe, F. P. Cammisa, Jr., *J. Spinal Disord.* **2000**, *13*, 422; e) C. Wimmer, H. Gluch, M. Franzreb, M. Ogon, *J. Spinal Disord.* **1998**, *11*, 124.
[4] a) J. B. Massie, J. G. Heller, J. J. Abitbol, D. McPherson, S. R. Garfin, *Clin. Orthop. Relat. Res.* **1992**, *284*, 99; b) J. S. Thalgott, H. B. Cotler, R. C. Sasso, H. LaRocca, V. Gardner, *Spine (Phila Pa 1976)* **1991**, *16*, 981.
[5] a) H. S. Gold, R. C. Moellering, Jr., *N. Engl. J. Med.* **1996**, *335*, 1445; b) A. D. Levi, C. A. Dickman, V. K. Sonntag, *J. Neurosurg.* **1997**, *86*, 975.

[6] A. Schwarz, in *The New York Times*, The New York Times Company, New York **2009**.
[7] a) T. E. Foster, B. L. Puskas, B. R. Mandelbaum, M. B. Gerhardt, S. A. Rodeo, *Am. J. Sports Med.* **2009**, *37*, 2259; b) N. E. Carlson, R. B. Roach, Jr., *J. Am. Dent. Assoc.* **2002**, *133*, 1383; c) D. Man, H. Plosker, J. E. Winland-Brown, *Plast. Reconstr. Surg.* **2001**, *107*, 229.
[8] E. K. Hartmann, T. Heintel, R. H. Morrison, A. Weckbach, *Arch. Orthop. Trauma. Surg.* **2010**, *130*, 909.
[9] a) J. Sys, J. Weyler, T. Van Der Zijden, P. Parizel, J. Michielsen, *Eur. Spine J.* **2011**, *20*, 1650; b) M. Scholz, P. Schleicher, T. Eindorf, F. Friedersdorff, M. Gelinsky, U. Konig, A. Sewing, N. P. Haas, F. Kandziora, *Spine (Phila Pa 1976)* **2010**, *35*, 740.
[10] D. J. Moojen, P. A. Everts, R. M. Schure, E. P. Overdevest, A. van Zundert, J. T. Knape, R. M. Castelein, L. B. Creemers, W. J. Dhert, *J. Orthop. Res.* **2008**, *26*, 404.
[11] T. M. Bielecki, T. S. Gazdzik, J. Arendt, T. Szczepanski, W. Krol, T. Wielkoszynski, *J. Bone Joint Surg. Br.* **2007**, *89*, 417.
[12] C. C. Trowbridge, A. H. Stammers, E. Woods, B. R. Yen, M. Klayman, C. Gilbert, *J. Extra Corpor. Technol.* **2005**, *37*, 381.
[13] S. J. Englert, T. H. Estep, C. C. Ellis-Stoll, *J. Extra Corpor. Technol.* **2005**, *37*, 148.
[14] T. Yuan, C. Zhang, B. Zeng, *Transfus. Apher. Sci.* **2008**, *38*, 167.
[15] a) S. Mehta, J. T. Watson, *J. Orthop. Trauma* **2008**, *22*, 432; b) G. Intini, *Biomaterials* **2009**, *30*, 4956.
[16] a) D. M. Donaldson, J. G. Tew, *Bacteriol. Rev.* **1977**, *41*, 501; b) R. R. Roberts, J. G. Tew, D. M. Donaldson, *Infect. Immun.* **1977**, *15*, 485; c) J. G. Tew, R. R. Roberts, D. M. Donaldson, *Infect. Immun.* **1974**, *9*, 179.
[17] a) R. L. Nachman, B. Weksler, *Ann. N. Y. Acad. Sci.* **1972**, *201*, 131; b) B. B. Weksler, R. L. Nachman, *J. Exp. Med.* **1971**, *134*, 1114.
[18] a) M. R. Yeaman, Y. Q. Tang, A. J. Shen, A. S. Bayer, M. E. Selsted, *Infect. Immun.* **1997**, *65*, 1023; b) M. R. Yeaman, S. M. Puentes, D. C. Norman, A. S. Bayer, *Infect. Immun.* **1992**, *60*, 1202; c) M. R. Yeaman, D. C. Norman, A. S. Bayer, *Antimicrob. Agents Chemother.* **1992**, *36*, 1665.
[19] M. R. Yeaman, *Clin. Infect. Dis.* **1997**, *25*, 951.
[20] J. Krijgsveld, S. A. Zaat, J. Meeldijk, P. A. van Veelen, G. Fang, B. Poolman, E. Brandt, J. E. Ehlert, A. J. Kuijpers, G. H. Engbers, J. Feijen, J. Dankert, *J. Biol. Chem.* **2000**, *275*, 20374.
[21] a) R. E. Marx, E. R. Carlson, R. M. Eichstaedt, S. R. Schimmele, J. E. Strauss, K. R. Georgeff, *Oral Surg. Oral Med. Oral Pathol. Oral Radiol. Endod.* **1998**, *85*, 638; b) B. L. Eppley, J. E. Woodell, J. Higgins, *Plast. Reconstr. Surg.* **2004**, *114*, 1502; c) R. Landesberg, A. Burke, D. Pinsky, R. Katz, J. Vo, S. B. Eisig, H. H. Lu, *J. Oral Maxillofac. Surg.* **2005**, *63*, 529; d) H. El-Sharkawy, A. Kantarci, J. Deady, H. Hasturk, H. Liu, M. Alshahat, T. E. Van Dyke, *J. Periodontol.* **2007**, *78*, 661.
[22] T. S. Roukis, T. Zgonis, B. Tiernan, *Adv. Ther.* **2006**, *23*, 218.
[23] H. B. Skinner, *Current diagnosis & treatment in orthopaedics, Fourth Edition*, The McGraw-Hill Companies, Inc, **2006**.
[24] D. H. Whitman, R. L. Berry, D. M. Green, *J. Oral Maxillofac. Surg.* **1997**, *55*, 1294.
[25] D. H. Whitman, R. L. Berry, *J. Oral Maxillofac. Surg.* **1998**, *56*, 1217.
[26] E. Anitua, *Int. J. Oral Maxillofac. Implants* **1999**, *14*, 529.
[27] L. J. Currie, J. R. Sharpe, R. Martin, *Plast. Reconstr. Surg.* **2001**, *108*, 1713.
[28] a) B. Li, B. Jiang, B. M. Boyce, B. A. Lindsey, *Biomaterials* **2009**, *30*, 2552; b) B. Li, B. Jiang, M. J. Dietz, E. S. Smith, N. B. Clovis, K. M. Rao, *J. Orthop. Res.* **2010**, *28*, 48; c) B. M. Boyce, B. A. Lindsey, N. B. Clovis, E. S. Smith, G. R. Hobbs, D. F. Hubbard, S. E. Emery, J. B. Barnett, B. Li, *J. Orthop. Res.* **2012**, *30*, 196.
[29] R. E. Marx, *J. Oral Maxillofac. Surg.* **2004**, *62*, 489.
[30] G. Weibrich, W. K. Kleis, G. Hafner, W. E. Hitzler, *J. Craniomaxillofac. Surg.* **2002**, *30*, 97.
[31] J. G. Hirsch, *J. Exp. Med.* **1960**, *112*, 15.
[32] J. Lonstein, R. Winter, J. Moe, D. Gaines, *Clin. Orthop. Relat. Res.* **1973**, *96*, 222.
[33] H. Li, H. Ogle, B. Jiang, M. Hagar, B. Li, *J. Orthop. Res.* **2010**, *28*, 992.
[34] K. A. Poelstra, N. A. Barekzi, D. W. Grainger, A. G. Gristina, T. C. Schuler, *Spine (Phila Pa 1976)* **2000**, *25*, 406.